Original Article
EPS8L3 promotes hepatocellular carcinoma proliferation and metastasis by modulating EGFR dimerization and internalization

Zefeng Xuan[1,2,3,4,5*], Long Zhao[1,2,3,4,5*], Zequn Li[1,2,3,4,5], Wenfeng Song[1,2,3,4,5], Jun Chen[1,2,3,4,5], Jian Chen[1,2,3,4,5], Hao Chen[1,2,3,4,5], Guangyuan Song[1,2,3,4,5], Cheng Jin[1,2,3,4,5], Mengqiao Zhou[1,2,3,4,5], Haiyang Xie[1,2,3,4,5], Shusen Zheng[1,2,3,4,5], Penghong Song[1,2,3,4,5]

[1]Division of Hepatobiliary and Pancreatic Surgery, Department of Surgery, First Affiliated Hospital, School of Medicine, Zhejiang University, Hangzhou 310003, China; [2]NHCPRC Key Laboratory of Combined Multi-organ Transplantation, Hangzhou 310003, Zhejiang Province, China; [3]Key Laboratory of The Diagnosis and Treatment of Organ Transplantation, CAMS, Hangzhou 310003, Zhejiang Province, China; [4]Key Laboratory of Organ Transplantation, Hangzhou 310003, Zhejiang Province, China; [5]Collaborative Innovation Center for Diagnosis Treatment of Infectious Diseases, Hangzhou 310003, Zhejiang Province, China. *Equal contributors.

Abstract: As a member of epidermal growth factor receptor (EGFR) kinase substrate 8 (EPS8) family, the role of EPS8 like 3 protein (EPS8L3) has not been well studied in malignancies. However, EPS8 has been reported to be associated with prognosis and functions in several kinds of cancers. Hence, whether EPS8L3 plays similar roles in the tumorigenesis of human cancers, especially in hepatocellular carcinoma (HCC), is still needed to be further explored. In this study, we revealed that EPS8L3 was overexpressed in HCC tissues compared with adjacent non-tumor tissues, and was associated with a poor clinical prognosis. Both *in vitro* and *in vivo* experiments showed that EPS8L3 could promote the proliferative ability by downregulating p21/p27 expression, and promote the migratory and invasive abilities by upregulating matrix metalloproteinase-2 expression. Furthermore, we demonstrated that EPS8L3 could affect the activation of the EGFR-ERK pathway by modulating EGFR dimerization and internalization, which may not depend on the formation of EPS8L3-SOS1-ABI1 complex. Taken together, our study showed that EPS8L3 plays a pivotal role in the tumorigenesis and progression of HCC, and it might be a potential therapeutic target for HCC.

Introduction

Hepatocellular carcinoma (HCC), the predominant form of liver cancer, is reported to be the fourth frequent cause of cancer related mortality worldwide, with over 800,000 newly diagnosed cases and over 700,000 deaths annually [1]. Surgical resection and liver transplantation were two main curative treatment for HCC patients in early stage, but the overall prognosis of HCC remains dismal for the late diagnosis or advanced stages [2]. Hence, it is urgent to explore novel molecular mechanisms about HCC initiation and progression, finding novel therapy targets and methods.

Epidermal growth factor receptor (EGFR) is a main member of the ERBB receptor family, which can be activated by EGF, transforming growth factor-α (TGFα), heparin-binding EGF, amphiregulin, betacellulin, epiregulin, epigen and neuregulin2-β [3]. Upon ligand binding to EGFR, receptors phosphorylation and activation of downstream signaling pathways were triggered by homodimerization or heterodimerization with other family members. As the major canonical downstream signaling pathways, RAS-RAF-MEK-ERK and RAS-PI3K-PTEN-AKT-mTOR can be subsequently activated, leading to the proliferation and migration of cancer cells [4]. Internalization of EGFR, which includes clathrin-mediated endocytosis and clathrin-independent endocytosis, also affect the transduction of signaling [5]. Anti-EGFR tyrosine kinase inhibitors (TKI) once were examples of

success in targeting oncogene addiction in cancer, but facing increasingly serious drug resistance due to tumor-specific adaptations [6, 7].

Epidermal growth factor receptor kinase substrate 8-like proteins (EPS8Ls), including EPS8, EPS8L1, EPS8L2 and EPS8L3, are originally found to be substrates for EGFR. Among them, EPS8 was firstly reported and relatively well studied, which contains several functional regions, including phosphotyrosine binding domain (PTB), EGFR-binding region, central SH3 domain and SAM-PNT domain overlapped by a C-terminal "effector region" [8]. The overexpression of EPS8 can be observed in various kinds of tumors, such as colon cancer, pancreatic cancer, ovarian cancer, breast cancer and oral cancer, affecting the processes of tumorigenesis, proliferation, migration and metastasis [9-15]. The other three family proteins conserve the major structure of EPS8, with different percentages of identical amino acids along the whole molecule [16]. Among them, EPS8L3 is the shortest in amino acid length and shares least similarity in modular organization with EPS8 (**Figure 1A**). The functions of EPS8L3 remains unknown, as it is only involved in a few studies, mainly focusing on Marie Unna hereditary hypotrichosis, lacking enough studies that related to tumorigenesis [17, 18].

In our study, we examined the expression of EPS8Ls family in HCC tumor tissues and matched normal tissues, and studied the function of EPS8L3 in HCC both *in vitro* and *in vivo*. Furthermore, the similarity and difference of the function with EPS8, and the relationship with EGFR were also explored.

Materials and methods

Patients and tissue samples

A total of 173 pairs of HCC tissue samples and 92 pairs of intrahepatic cholangiocarcinoma (ICC) tissue samples were collected from patients who underwent curative surgical resection of HCC or ICC as primary treatment at the Department of Hepatobiliary Surgery, First Affiliated Hospital of Zhejiang University (Zhejiang, China). Paraffin-embedded HCC samples from 114 patients were used to construct tissue microarrays (TMAs) for immunohistochemistry (IHC) staining (Servicebio, Wuhan, China). Fresh frozen samples were used for quantitative real-time polymerase chain reaction (qRT-

PCR) and western blot analysis. The study was approved by the First Affiliated Hospital of Zhejiang University Ethics Committee, and written informed consent was obtained from each patient in this study.

Cell lines and cell culture

Four liver cancer cells, including SNU449, HepG2, HCCLM3 and Huh7 were purchased from the China Center for Type Culture Collection (CCTCC, Wuhan, China). All cell lines had been authenticated using STR profiling. Cell lines were cultured in MEM or 1640 (Gibco, USA) supplemented with 10% (vol/vol) fetal bovine serum (FBS, Gibco) in a humidified incubator with 5% CO_2 at 37°C.

Small interference RNAs and stable cell clones establishment

Small interference RNAs (siRNAs) targeted to EPS8 and EPS8L3 mRNA were applied to knockdown endogenous EPS8 and EPS8L3 (Table S1). siRNAs were delivered into cells by using lipofectimine 2000 (Thermo Fisher Scientific, USA). Lentiviruses containing the complete open reading frame of EPS8L3 (Vector-EPS8L3) and lentiviral-based small hairpin RNA (shRNA) targeting EPS8L3 (shRNA-EPS8L3) were purchased from Funeng Company (Guangzhou, China). Vector-NC and shRNA-NC were used as negative controls. The target sequences of shRNA-EPS8L3 were listed in Table S2. Puromycin with a final concentration of 5 µg/mL was used for the selection of transfected cells, and the selected cells were considered as stable cell clones which could be prepared for subsequent experiments.

RNA isolation and qRT-PCR

Total RNA of tissues and cultivated cells was extracted using TRIzol Reagent (Thermo Fisher Scientific) according to the manufacturer's instructions. Complementary DNA was synthesized using HiScript II 1st Strand cDNA Synthesis Kit (Vazyme, Nanjing, China). qRT-PCR was carried out using ChamQ Universal SYBR qPCR Master Mix (Vazyme) and 7500HT Fast Real-Time PCR System (Applied Biosystems, USA). The primers for qRT-PCR were shown in Table S3. Relative gene expressions were normalized to the expression of glyceraldehyde-3-phosphate dehydrogenase (GAPDH) as an internal control.
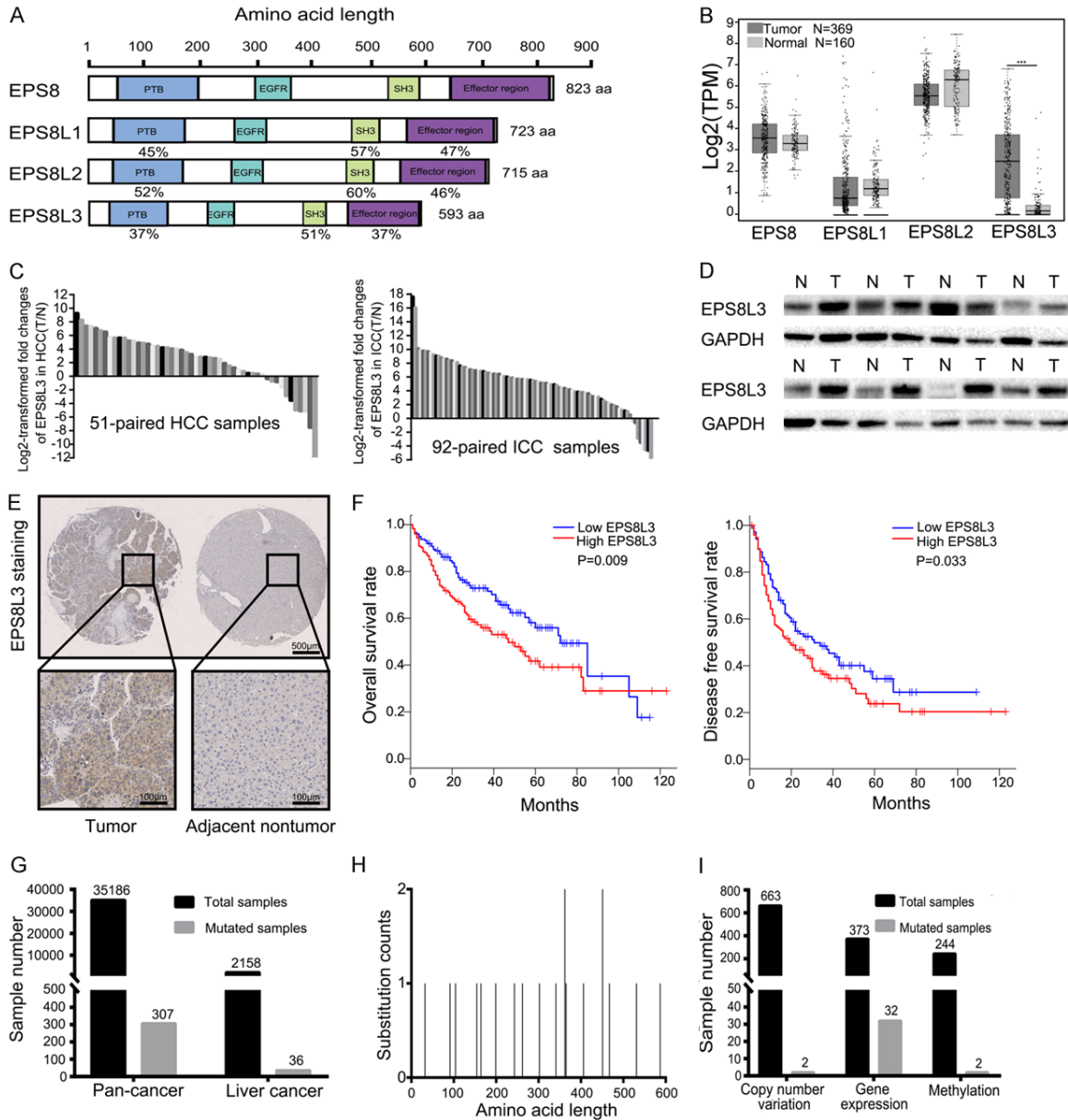
Figure 1. Upregulation of EPS8L3 expression in human tumor tissues. A. Schematic representation of human EPS8 and three related proteins EPS8L1, EPS8L2 and EPS8L3. B. The mRNA expression of EPS8, EPS8L1, EPS8L2 and EPS8L3 of human liver tissues in TCGA and GTEx databases (Number of tumor tissues = 369; Number of normal tissues = 160). C. The mRNA expression of EPS8L3 was detected in 51-paried (HCC) and 92-paried (ICC) tumor tissues and adjacent non-tumorous tissues by RT-qPCR. D. The protein levels of EPS8L3 were examined by western blotting in 8-paired HCC tissues. E. Representative images of IHC for EPS8L3 expression in tumor tissues and adjacent non-tumor tissues of HCC patients (N = 114). F. HCC patients with low EPS8L3 mRNA expression exhibited better overall survival rate and disease free survival rate in GEPIA database (N = 182 per group). G. Total samples tested and samples with EPS8L3 point mutations in pan-cancer and liver cancer. H. Graphical view of point mutations across EPS8L3 in liver cancer samples. Mutations are displayed at the amino acid level across the full length of the gene. I. Total samples tested and samples with EPS8L3 variants, including copy number variation, gene overexpression and methylation.

Western blot analysis

Total protein of cells or tissues was extracted by using RIPA buffer (Thermo Fisher Scientific) containing proteinase inhibitor (cocktail, Thermo Fisher Scientific). Cell lysates were separated by SDS-PAGE gels (GenScript, Nanjing, China) and transferred onto polyvinylidene

difluoride (PVDF) membranes (Millipore, USA). The membranes were blocked with 5% nonfat milk at room temperature for 1 h, and incubated with their respective primary antibodies and HRP-conjugated secondary antibodies. The antibodies used in western blot analysis were listed in Table S4. The chemiluminescent signaling was detected by using ECL chemiluminescence detection kit (Millipore).

Immunohistochemistry analysis

Paraffin-embedded tissues were cut into slices, mounted on slides, deparaffinized and rehydrated. 3% H_2O_2 in methanol was used to inactivate endogenous peroxidase activity, and citrate buffer was applied to retrieve antigen in a microwave oven. Then, the slices were exposed to indicate primary antibodies overnight at 4°C. In the next day, the slices were incubated with corresponding secondary antibodies before staining with DAB (Zsbio, Beijing, China). The antibodies used in immunohistochemistry were listed in Table S4. Stained tissue sections were assessed manually by two independent pathologists without knowledge of the patients' clinical characteristics, and the method for staining score has been introduced in our previous study [19].

Immunofluorescence

Cells grown on confocal cell culture dishs (Nest, CA, USA) were washed with fixed with 4% paraformaldehyde for 15 min. After blocking with 4% bovine serum albumin (BSA) and permeabilizing with 0.5% Triton-X, the cells were incubated with primary antibodies overnight at 4°C. After washing with phosphate buffer saline (PBS), the cells were incubated with Alexa Fluor 488 and Alexa Fluor 594 labeled IgG (Thermo Fisher Scientific) for an hour. After washing again, the cells were stained with DAPI (Thermo Fisher Scientific) for 5 min, and imaging was taken with a high-resolution confocal microscope (Olympus, Japan). For the experiment of internalization of EGFR, the serum-starved cells were stimulated with EGF for 15 min before fixed with 4% paraformaldehyde. Antibodies used in immunohistochemistry were listed in Table S4.

Cell proliferation assay

Cell proliferation assay was performed with cell counting kit-8 (CCK-8, Dojindo, Japan). In brief, cells were seeded into 96-well plates with 2000 cells per well and cultured in MEM or 1640 with 10% FBS. CCK-8 reagent was added at different time points. Optical density was measured by microtiter reader (Biotek, Winooski, USA) at 450 nm. Relative cell numbers were normalized to the cell numbers of first day based on the optical density.

Colony formation assay

Cells were plated in 6-well plates (2000 cells per well) and cultured for about two weeks. The plates were stained with 1% crystal violet after being fixed in 4% paraformaldehyde for 30 min. The numbers of colonies in every well were counted to evaluate the ability of colony formation.

Cell migration and invasion analysis

Transwell chambers (Millipore) with polycarbonate membranes (8 μm pore size) were used in this study. Serum-free MEM or 1640 containing 2×10^4 cells were added to the upper chamber, while MEM or 1640 containing 10% FBS was added to the bottom chamber. Filters were precoated with 60 μl Matrigel (BD Biosciences, USA) for invasion assays. The migrated or invaded cells on the outside of filter membrane were fixed and stained with crystal violet for 30 min at room temperature. The numbers of cells on the outside of membrane were counted to evaluate the ability of migration or invasion.

Wound healing assay

The wound healing assay was performed by using the culture-inserts 2 well for self-insertion (ibidi, Martinsried, Germany). Cells were seeded into the wells and cultured for one day. Cell-free gaps were created by removing the culture-inserts after cell attachment. Images were obtained by a microscope (Olympus) at 0 h and 48 h after the removal.

Flow cytometry analysis

For cell cycle analysis, cells were trypsinized and fixed with cold 70% ethanol at -20°C overnight. In the next day, cells were collected and stained with propidium iodide (BD Bioscience, USA) for 15 min in dark at room temperature. After that, cell cycle analysis was performed by FACS flow cytometer (BD Bioscience).

For EGFR internalization assay, cells were serum-starved for two days before the assay. On

the third day, cells were collected after incubating with EGF (Peprotech, NY, USA) for 15 min or not. Then the cells were incubated with Alexa Fluor 488 anti-human EGFR antibody (#352908, Biolegend, CA, USA) without permeation for 30 min in dark. After washing with PBS, cells were promptly subjected to the flow cytometry analysis. For cell stemness assay, cells were incubated with PE anti-human CD133 antibody (#372803, Biolegend, CA, USA) and FITC anti-human CD326 antibody (#324204, Biolegend, CA, USA).

Dimerization of EGFR

Cells were grown in MEM with 10% FBS and then were serum-starved for two days before treating with EGF (100 ng/ml). Cells were cross-linked by BS3 (Thermo Fisher Scientific) with a concentration of 2.5 mM at room temperature for 30 min at the designated time (0 and 15 min) after EGF stimulation. Tris-HCl (pH = 7.5) with a concentration of 10 mM was used to quench the cross-link. And then western blot analysis was performed to detect EGFR dimerization in those cells.

Animal experiments

Four-week-old male BALB/c nude mice were purchased from Shanghai Experimental Animal Center of Chinese Academy of Sciences and fed in a pathogen-free vivarium. HCCLM3 cells (3×10^6) with stable transfection were injected subcutaneously into the armpits of nude mice for subcutaneous xenograft study, and injected into caudal vein for pulmonary colonization assay. Tumor size was calculated with the formula: volume = 1/2 × (long diameter) × (short diameter)^2. When the largest tumor volume reached approximately 1 cm^3, all tumors were excised, photographed and weighted. For orthotopic transplantation tumor model, HCC tissues from subcutaneous transplanted tumor model were injected (1 mm^3) into the livers. For pulmonary colonization assay, small living animal imaging technology was applied with the use of D-luciferin sodium salt (Yeasen, Shanghai, China). Both the tumors and lungs were fixed in 4% paraformaldehyde and applied to IHC analysis. All animal studies were designed in accordance with the National Institutes of Health Animal Care and Use Guidelines and approved by the Animal Care Committee of Zhejiang University.

Statistical analysis

Statistical analyses were performed with SPSS 23.0 for Windows (SPSS Inc., IL, USA). The difference between experimental groups was compared using Student t-test and Chi-square analysis. The survival rates were analyzed by Kaplan-Meier survival analysis. Graphs were made using GraphPad Prism software (GraphPad Software Inc., CA, USA). Data are expressed as mean ± standard deviation (SD). A *p* value <0.05 was considered to be statistically significant.

Results

Expression of EPS8L3 is frequently upregulated in human tumor specimens

The mRNA expressions of EPS8 family were detected in liver tumor tissues and normal tissues in TCGA and GTEx databases. Among them, only the mRNA expression of EPS8L3 was much higher in tumor tissues than in normal tissues (**Figure 1B**). EPS8 mRNA expression had been reported to be upregulated in many kinds of tumor tissues, but it failed to be upregulated in HCC tissues. In order to explore whether there were some correlations between the mRNA expression of EPS8L3 and other family members, we performed a correlation analysis using TCGA data. The result revealed that no significant corrections were existed (Figure S1A-C).

In addition, the mRNA expression of EPS8L3 were evaluated in other kinds of human tumor comparing with respective normal tissues, which demonstrated that the expressions were increased in cholangiocarcinoma (CHOL), colon adenocarcinoma (COAD), esophageal carcinoma (ESCA), pancreatic adenocarcinoma (PAAD) and rectum adenocarcinoma (READ) (Figure S1D). The RT-qPCR results using 51 pairs of fresh HCC samples and 92 pairs of fresh ICC samples further confirmed the former findings (**Figure 1C**). Results from western blotting analysis of 8-paired HCC samples and IHC staining using tissue microarrays assay also demonstrated that tumor samples had higher EPS8L3 level than that in adjacent non-tumorous samples (**Figure 1D**, **1E**). More importantly, EPS8L3 expression was significantly associated with pathological differentiation (P = 0.003) (**Table 1**). Furthermore, patients with lower EPS8L3 mRNA expression exhibited better overall sur-

Table 1. Correlation between clinicopathological features of HCC patients and EPS8L3 expression

Variation	Relative EPS8L3 expression in HCC (tumor/adjacent non-tumor)		
	Low (≤1, n = 69)	High (>1, n = 45)	*P* value
Gender			
Male	65	41	0.528
Female	4	4	
Age (years)			
≥40	56	39	0.441
<40	13	6	
Tumor size (diameter)			
≥5 cm	50	33	0.919
<5 cm	19	12	
Tumor number			
Single	55	37	0.740
Multiple	14	8	
Cirrhosis			
Yes	56	35	0.660
No	13	10	
AFP Level (ng/ml)			
≥400	22	15	0.872
<400	47	30	
Vascular invasion			
Yes	22	21	0.111
No	47	24	
Tumor thrombosis			
Yes	41	29	0.590
No	28	16	
TNM stage			
I-II	57	34	0.359
III-IV	12	11	
Pathological differentiation			
I-II	56	25	0.003**
III-IV	13	20	

Abbreviations: AFP, alpha-fetoprotein; EPS8L3, epidermal growth factor receptor kinase substrate 8-like protein 3; HCC, hepatocellular carcinoma; TNM, tumor/node/metastasis. **: P<0.01.

vival rate (P = 0.009) and disease free survival rate (P = 0.033) (**Figure 1F**). In order to explore the possible mechanism for the overexpression of EPS8L3 at mRNA level in tumor tissues, we analyzed the mutations of EPS8L3 in both pan-cancer and liver cancer using the COSMIC database. According to the analysis, EPS8L3 has a low rate of point mutation, copy number variation and methylation, but has a relatively high rate of gene overexpression (**Figure 1G-I**, Figure S1E-G).

EPS8L3 contributes to HCC cell proliferation

To explore the potential functions of EPS8L3 in HCC, we performed the gain or loss-of-function studies in HCCLM3, Huh7, HepG2 and SNU449 cells. Lentiviruses and siRNAs were applied to change the mRNA expression of EPS8L3. The EPS8L3 mRNA expressions were significantly decreased in knockdown groups comparing with normal control group, while the mRNA expressions of three other family members were not obviously changed. Meanwhile, the EPS8L3 mRNA expressions in the overexpression groups increased with other members unchanged (**Figure 2A**, **2B**). Remarkable decrease or increase of EPS8L3 expression could be observed by western blotting after the respective lentiviruses transfection in both HCCLM3 and Huh7 cells (**Figure 2A**, **2B**).

Compared with respective control cells, EPS8L3 knockdown cells showed obvious decrease in cell growth rate, while EPS8L3 overexpressed cells exhibited significant increase in cell growth rate by CCK-8 assay (**Figure 2C**, **2D**). Furthermore, colony formation assay was applied to assess the effect of EPS8L3 on colony formation ability both in HCCLM3 and Huh7 cells. Colony number of EPS8L3 depleted cells was decreased and that of EPS8L3 overexpressed cells was increased compared to their respective control cells (**Figure 2E**, **2F**). In addition, flow cytometry assay was carried out to assess the effect of EPS8L3 knockdown and overexpression on cell cycle. An obvious increase of cells in G0/G1 phase and a significant reduction of cells in G2/M phase was observed in the knockdown group comparing with its control group. On the contrary, the relative cell number in G0/G1 phase significant decreased and that in G2/M phase obvious increased in overexpression group comparing with control group (**Figure 2G**, **2H**). The role of EPS8L3 in promoting cell proliferation was further confirmed in HepG2 and SNU449 (Figure S2A-D). Collectively, these
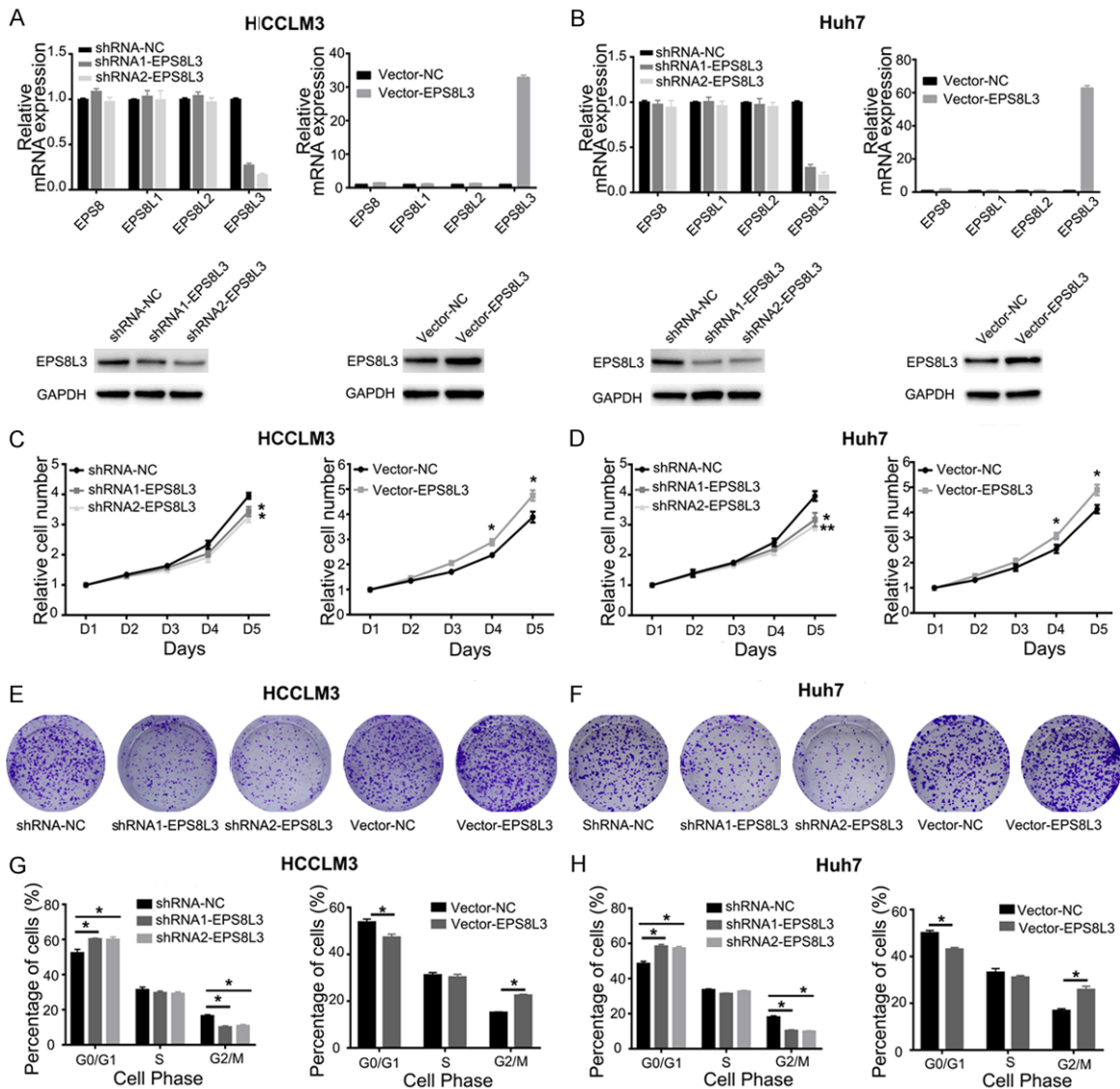
Figure 2. Changes of cell proliferation after EPS8L3 knockdown and overexpression in HCC cells. (A, B) The relative mRNA expressions of EPS8Ls family and protein expression of EPS8L3 after EPS8L3 knockdown or overexpression in HCCLM3 (A) and Huh7 (B) cells. (C, D) Cell growth was inhibited after the knockdown of EPS8L3, but promoted after the overexpression of EPS8L3 in HCCLM3 (C) and Huh7 (D) cells. (E, F) Colony formation of HCCLM3 (E) and Huh7 (F) cells after EPS8L3 knockdown or overexpression. (G, H) Cell cycle distribution was detected after the knockdown or overexpression of EPS8L3 in HCCLM3 (G) and Huh7 (H) cells. Quantitative data were shown as mean ± s.d. Results were obtained from three independent experiments. *: P<0.05, **: P<0.01.

data showed that knockdown or overexpression of EPS8L3 effectively inhibited or promoted cell proliferation, which might imply that EPS8L3 played an important role in cell proliferation.

EPS8L3 promotes HCC cell migration and invasion

As EPS8 has been reported to affect cell migration and invasion in many kinds of tumor, we used transwell models and wound healing

assays to verify whether EPS8L3 had similar effects in HCC cell lines. The abilities of migration and invasion were obviously inhibited in knockdown group, while they were significantly promoted in overexpression group comparing with their respective control groups in Huh7, HepG2 and SNU449 cells (**Figures 3A**, <u>S2E</u>, <u>S2F</u>). Wound healing assays also demonstrated that the migratory ability was weakened after the knockdown of EPS8L3 in four HCC cell lines, and the changes were most obvious in Huh7 cell lines (**Figures 3B**, <u>S2G</u>, <u>S2H</u>). Con-
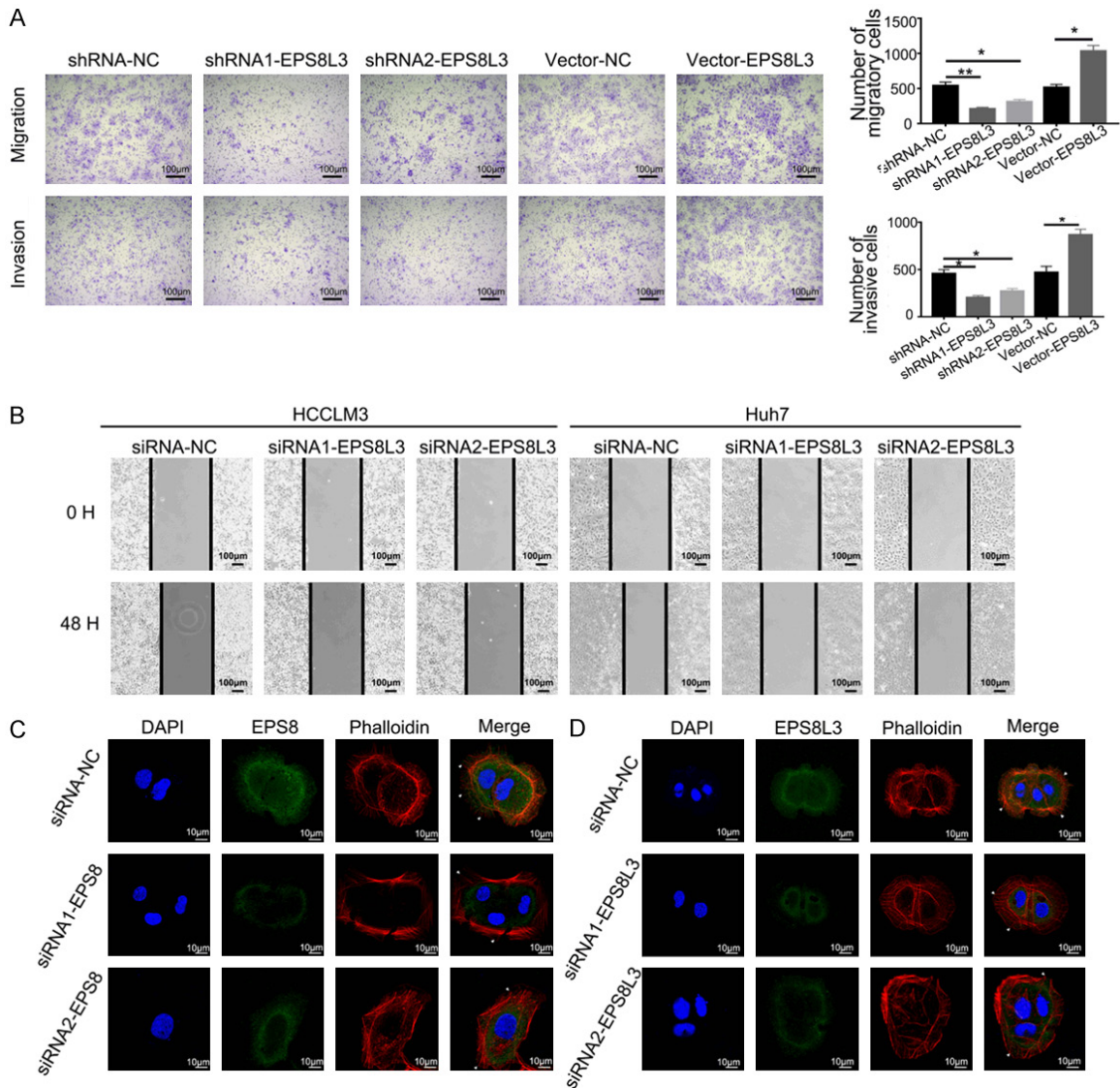
Figure 3. EPS8L3 promoted cell migration and invasion of HCC *in vitro*. (A) The migratory and invasive abilities of Huh7 cells were evaluated by transwell-assays. Representative images were shown in left panel. The numbers of migratory or invasive cells in different groups were shown in the right panel. (B) Representative images of wound healing assay. The cell-free gap was much narrower in the negative control group than in the EPS8L3 knockdown groups. (C, D) Representative images showing the changes of F-actin and pseudopodia after EPS8 (C) or EPS8L3 (D) knockdown in Huh7 cells. Results of three independent experiments were shown as mean ± s.d. *: P<0.05, **: P<0.01.

sidering that EPS8 played an important role in controlling actin capping and bunding in the formation of filopodia, we supposed that EPS8L3 may have similar functions on actin capping and bunding. HCC cell lines were transfected with two independent EPS8-specific or EPS8L3-specific siRNAs, and the mRNA expression changes of EPS8 family genes were detected. The results revealed that the specific siRNAs could specifically decrease the target gene,

and make other three members unchanged (Figure S3A, S3B). After the confirmation of siRNA efficacy, we performed immunofluorescence to evaluate the role of EPS8L3 on actin and filopodia formation in Huh7 cells. The filopodia turned out to be much less in the EPS8 knockdown groups comparing with its normal control group, while the difference was not so obvious between EPS8L3 knockdown groups and control group (**Figure 3C**, **3D**).

Whether epithelial-mesenchymal transition (EMT) and cell stemness were involved in the change of migratory and invasive abilities, we checked the expressions of several EMT, cell stemness and hepatic differentiation related markers in EPS8L3 knockdown cells and control cells. No significant differences were observed between two groups at the mRNA level (Figures S3C-F, S4A-D). The protein expression of E-cadherin was increased, while N-cadherin and Vimentin were decreased in EPS8L3 knockdown HCCLM3 cells, but the similar changes were not observed in Huh7 cells (Figure S3G). The expressions of CD133 and CD326 were turned out to be similar between the knockdown groups and control groups (Figure S4E-H). In total, EMT might be involved in the change of migratory and invasive abilities, but cell stemness might not be affected by the knockdown of EPS8L3.

EPS8L3 enhances the activation of the EGFR-ERK pathway

As the EPS8Ls family was EGFR pathway substrates, we supposed that EPS8L3 might promote HCC cells proliferation and metastasis through activating the EGFR-ERK pathway, which was considered to be one of the major canonical pathways that could be activated by EGFR. For this purpose, the activation of EGFR and downstream molecules in EPS8L3 knockdown HCC cells were examined. The results revealed that EGFR phosphorylation (pEGFR) at Y1068 residues and ERK phosphorylation (pERK) were reduced in EPS8L3 knockdown cells in comparison to those in control cells, and the protein levels of intermediate molecules, mainly including Raf-1 phosphorylation (pRaf-1) and MEK1 phosphorylation (pMEK1), were both decreased to some extent (**Figure 4A**, **4B**). Moreover, the decreased matrix metalloproteinase-2 (MMP2) expression and increased p21/p27 expression were also observed in knockdown group, when compared to control groups, but the change of matrix metalloproteinase-9 (MMP9) was not obvious enough (**Figure 4C**). The IHC staining of p21 and p27 using the TMAs confirmed that both of them had relatively lower protein expressions in the tumor tissues than in adjacent nontumor tissues. Meanwhile, the correlations between EPS8L3 and p21 or p27 were analyzed based on the IHC staining scores, and the results

revealed that significant negative correlation existed between EPS8L3 and p21, but not between EPS8L3 and p27 (**Figure 4D**, **4E**). Taken together, our study demonstrated that EPS8L3 could regulate the EGFR-ERK pathway.

EPS8L3 knockdown inhibited the dimerization and internalization of EGFR

Dimerization and internalization of EGFR are two crucial steps in the EGFR-mediated signal transduction. Whether EPS8L3 could modulate the EGFR-ERK pathway via these two steps was still needed to be further verified. Thus, dimerization and internalization of EGFR in EPS8L3 knockdown HCC cells was examined. The formation of EGFR dimers after EGF stimulation appeared to be less effective in EPS8L3 knockdown HCC cells compared with negative control cells (**Figure 5A**). As EGFR internalization also played a pivotal role in the downstream signal transduction and receptor recycling, it was also explored by flow cytometry and immunofluorescence. EGFR on cell surface was measured by flow cytometry to reflect EGFR internalization. With the deletion of EPS8L3, level of EGFR on cell surface was dramatically increased in response to EGF stimulation (**Figure 5B**). Moreover, the percentages of colocalization between EGFR and EEA1, an early endosome marker that representing EGFR internalization, were obviously reduced in EPS8L3 knockdown Huh7 cells after EGF stimulation comparing with the control cells (**Figure 5C**, **5D**). In summary, these results showed that loss of EPS8L3 could significantly impair the dimerization and internalization of EGFR.

As the functions of EPS8 were mainly depended on the formation of EPS8-ABI1-SOS1 complex, the role of the complex in EPS8L3 related functions was still unclear. Significant positive correlations were existed among EPS8, SOS1 and ABI1 at the mRNA level (**Figure 6A-C**). However, no significant correlations were observed between EPS8L3 and SOS1 or ABI1 at the mRNA level (**Figure 6D**, **6E**). Although the protein expressions of SOS1 and ABI1 in HCC tissues were both much higher than in adjacent non-tumorous tissues, which was consistent with the protein expression of EPS8L3, but the correlations were still weak at the protein level (**Figure 6F**, **6G**). Hence, EPS8L3 might affect
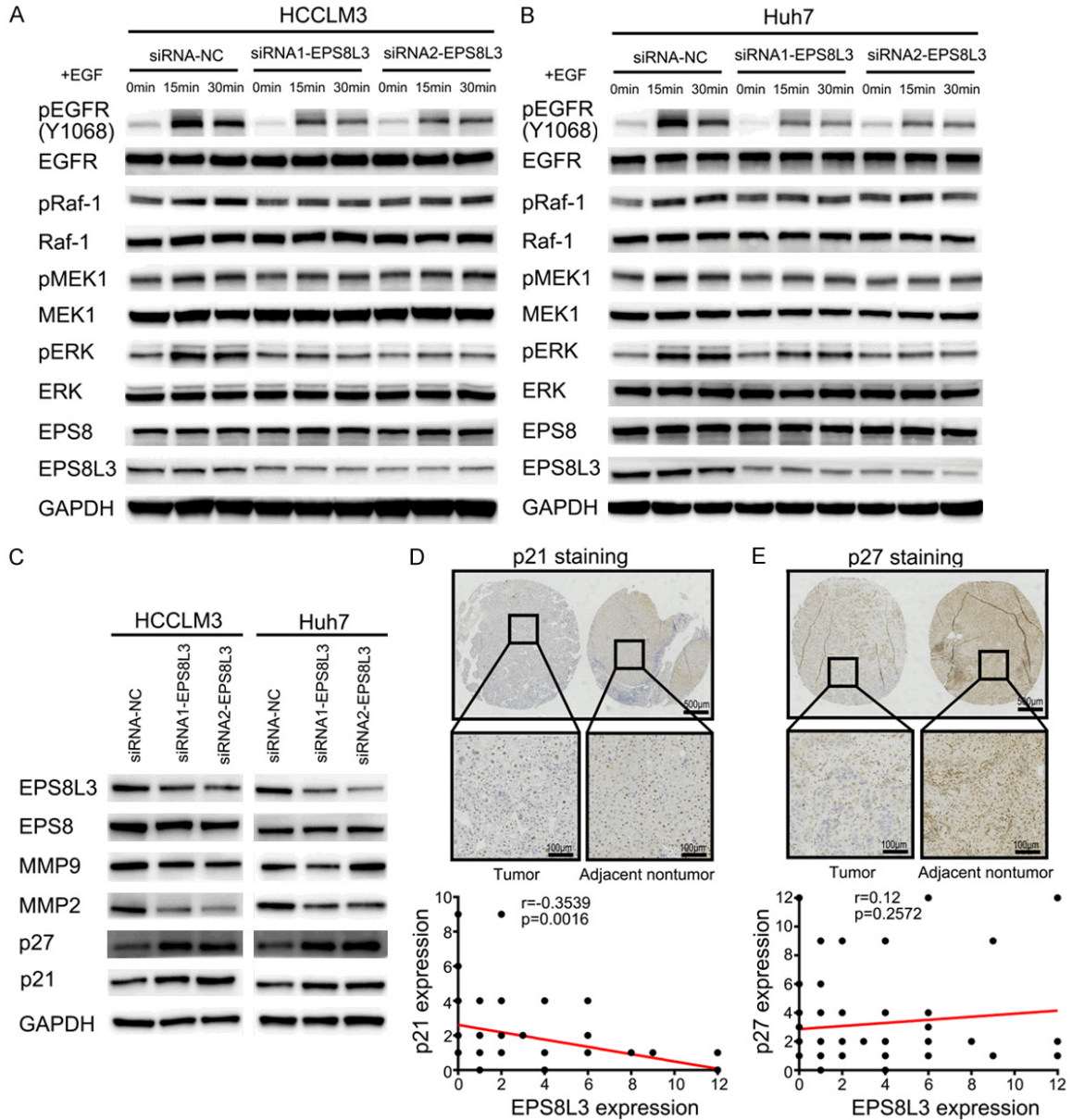
Figure 4. Repression of the EGFR-ERK pathway after EPS8L3 knockdown in HCC cells. (A, B) The changes of related protein levels in the EGFR-ERK pathway after EPS8L3 knockdown in HCCLM3 (A) and Huh7 (B) cells. (C) The change of MMP2, p21 and p27 in HCCLM3 and Huh7 cells with EPS8L3 knockdown. (D, E) Representative images of IHC for p21 (D) and p27 (E) expression in tumor tissues and adjacent non-tumor tissues of HCC patients (N = 114). The correlations between EPS8L3 and p21 or p27 were shown in the bottom panel.

the dimerization and internalization of EGFR through a complex-independent way in HCC.

EPS8L3 promotes tumor growth and pulmonary colonization in mice

To investigate the role of EPS8L3 in tumor growth and pulmonary colonization *in vivo*, EPS8L3 knockdown or overexpressed HCCLM3 cells together with negative control cells were injected subcutaneously into nude mice for

growth analysis and through caudal vein for pulmonary colonization analysis. Orthotopic transplantation tumor model was also established using HCC tissues from subcutaneous transplanted tumor model. Subcutaneous tumor size was measured every 4 or 6 days and tumors were weighed after excision. Both tumor volume and tumor weight were significantly decreased in the EPS8L3 knockdown groups, while obviously increased in the overexpression group compared with their respective con-
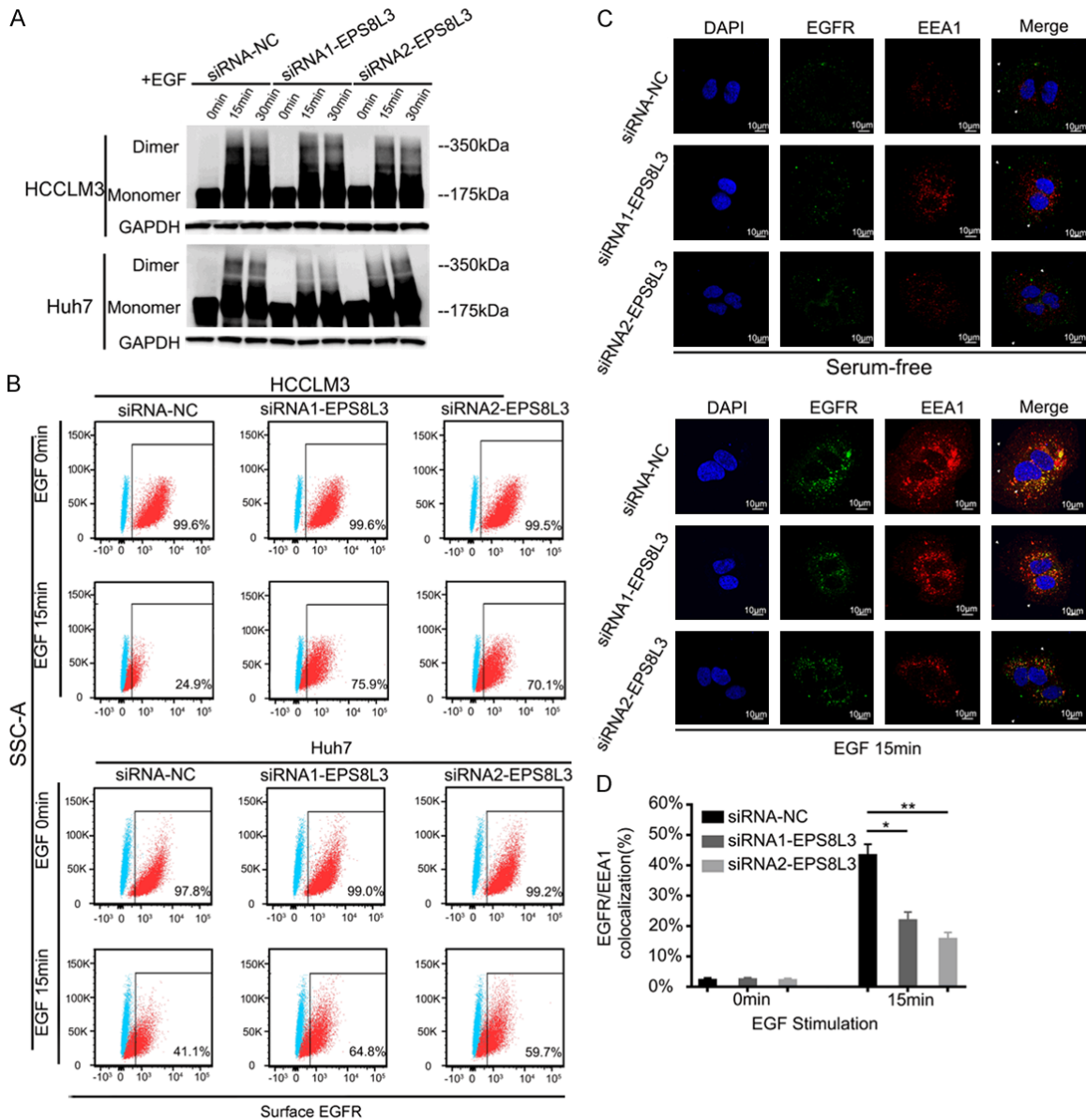
Figure 5. Blockade of dimerization and internalization of EGFR in EPS8L3 knockdown HCC cells. A. The dimer and monomer form of EGFR were evaluated in negative control cells and EPS8L3 knockdown cells. B. The percentages of EGFR on cell surface were evaluated by flow cytometry in the presence or absence of EGF (100 ng/ml). C. EPS8L3 knockdown Huh7 cells and negative control cells incubated with or without EGF (100 ng/ml) for 15 min were subjected to the immunofluorescence assay. Representative pictures were shown. D. The percentages of co-localization of EGFR and EEA1 were calculated. Results of three independent experiments were shown as mean ± s.d. *: P<0.05, **: P<0.01.

trol groups (**Figure 7A, 7B**). Meanwhile, the results from orthotopic transplantation tumor model demonstrated that both tumor weight and tumor weight/liver weight ratio were increased in EPS8L3 overexpression group (**Figure 7C**). The difference of pulmonary colonization between different groups was measured by small living animal imaging technology. The

percentage of mice with lung colonization was much higher in the control group in comparison with EPS8L3 knockdown groups (**Figure 7D**). Hematoxylin-eosin staining of lungs also revealed that the tumor in the control group was bigger than those in knockdown groups (**Figure 7E**). With the reduction of EPS8L3, the protein levels of Ki-67 and MMP2 were reduced signifi-
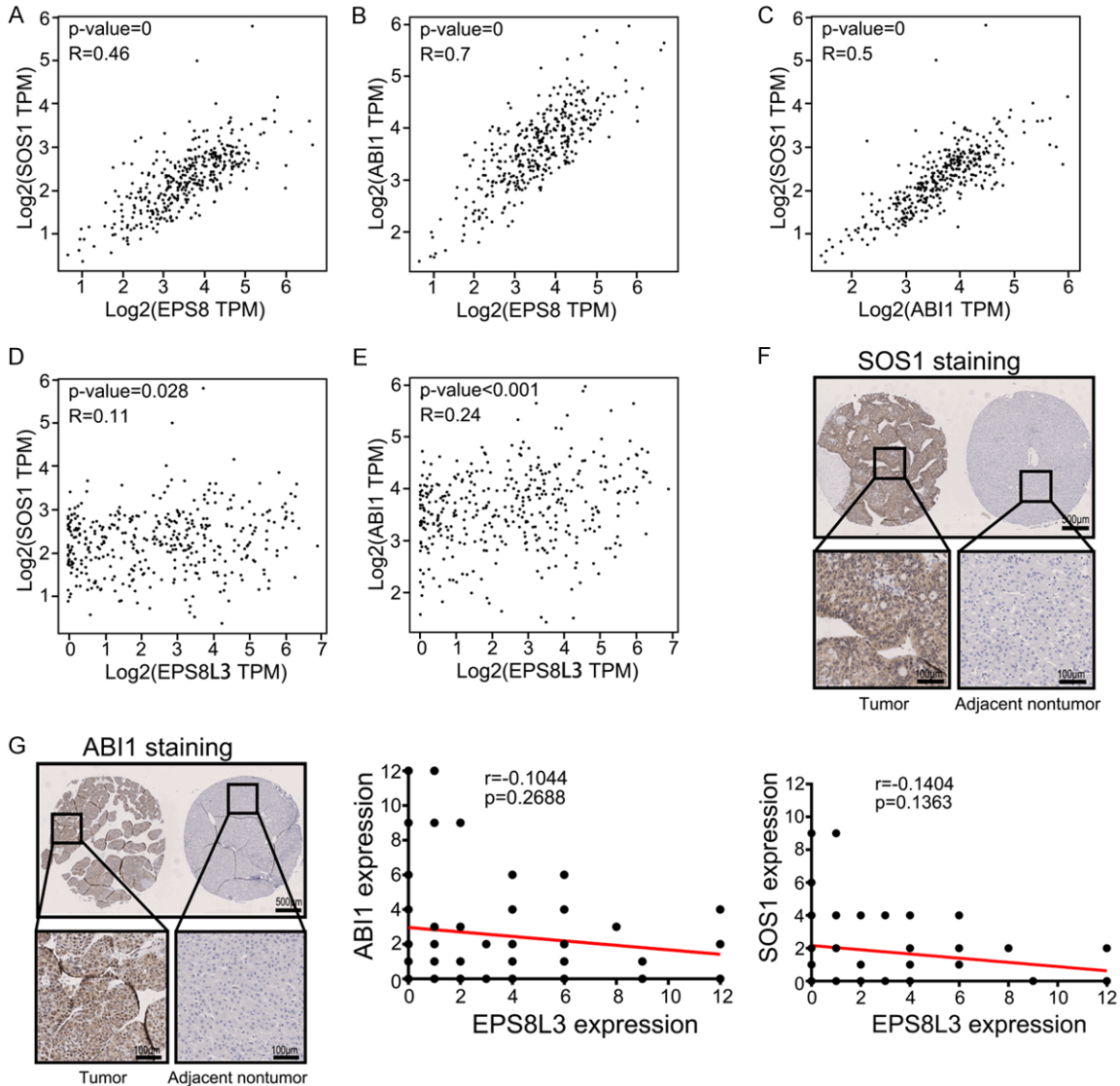
Figure 6. The correlation between the expression of EPS8, EPS8L3, SOS1 and ABI1. A-C. The correlation between the mRNA expression of EPS8, SOS1 and ABI1 of human HCC tissues in TCGA database (N = 369). D, E. The correlation between the mRNA expression of EPS8L3, SOS1 and ABI1 of human HCC tissues in TCGA database (N = 369). F. Representative images of IHC for SOS1 expression in tumor tissues and adjacent non-tumor tissues of HCC patients (N = 114). The correlation between EPS8L3 and SOS1 was shown in the bottom panel. G. Representative images of IHC for ABI1 expression in tumor tissues and adjacent non-tumor tissues of HCC patients (N = 114). The correlation between EPS8L3 and ABI1 was shown in the right panel.

cantly as evident by IHC analysis. Contrarily, the protein levels of Ki-67 and MMP2 were increased with the overexpression of EPS8L3 (**Figure 7F**). Accordingly, EPS8L3 could promote tumor growth and pulmonary colonization *in vivo*.

Discussion

EGFR, which belongs to receptor tyrosine kinases (RTKs), is regarded as a promising therapeutic target for various kinds of cancer. With the clinical application of TKIs, patients with tumors including non-small cell lung cancer (NSCLC), breast cancer and renal cell carcinoma, showed better survival rates [20-22]. However, in term of HCC, treatment failure was reported in related clinical trials, partly due to the incomplete understanding of the underlying mechanism that drives tumor progression [23]. EPS8, a substrate for EGFR, has been reported to be upregulated in many kinds of cancer and cor-
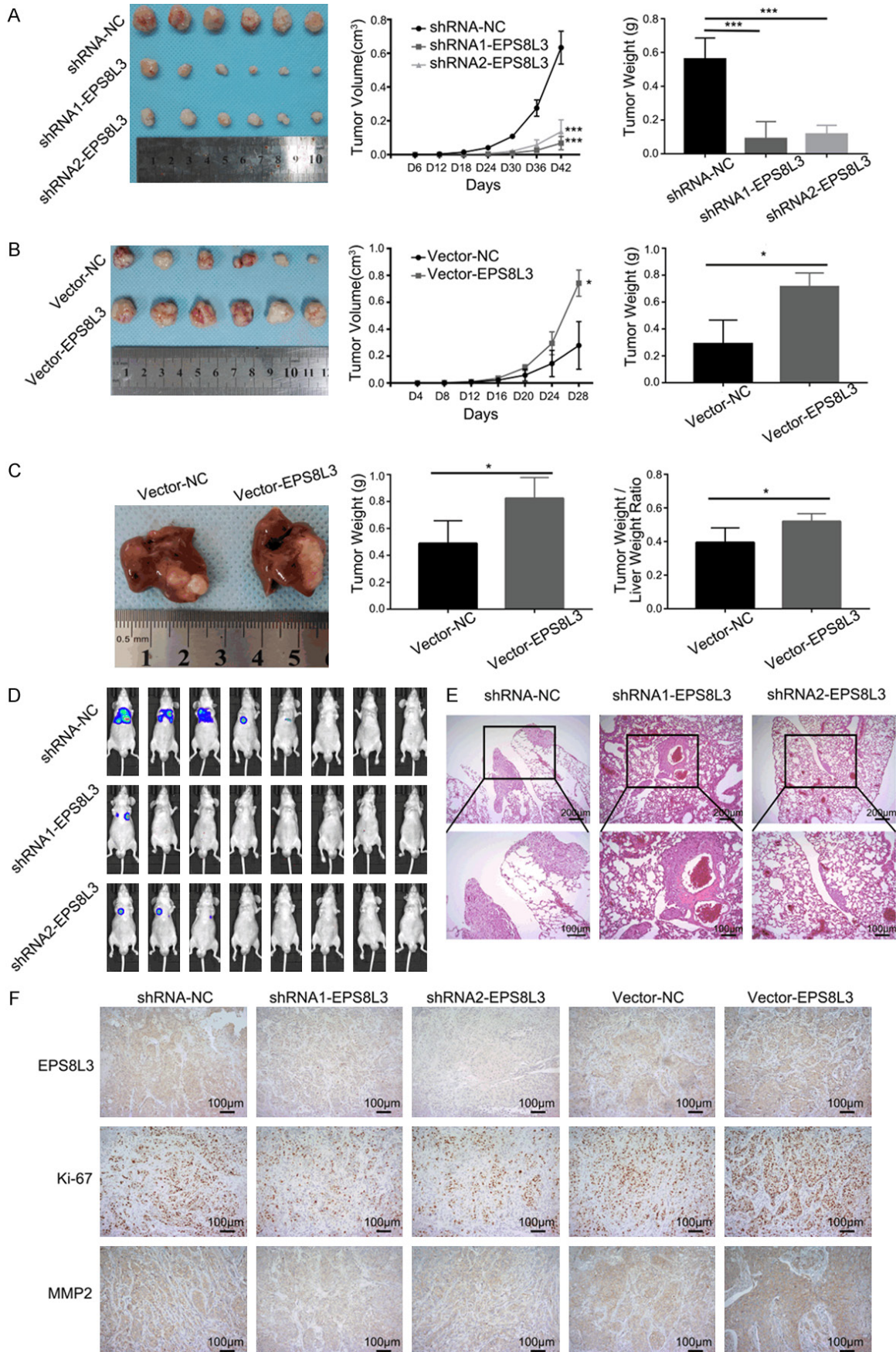
Figure 7. Changes of proliferation and pulmonary colonization with EPS8L3 alteration. A. Tumor growth of EPS8L3 knockdown HCCLM3 cells and negative control cells was measured every 6 days. Tumors were weighed after excision (N = 6). B. Tumor growth of EPS8L3 overexpressed HCCLM3 cells and negative control cells were measured every 4 days. Tumors were weighed after excision (N = 6). C. Representative tumors from orthotopic transplantation tumor model were shown. Tumors and livers were weighed after excision (N = 5). D. The images of small living animal imaging using D-luciferin sodium salt were shown. (N = 8 per group). E. Representative pictures of pulmonary colonization foci in different groups. F. Representative pictures of IHC staining for different groups were displayed. Results of three independent experiments were shown as mean ± s.d. *: P<0.05, **: P<0.01, ***: P<0.001.

related with tumorigenesis, proliferation and metastasis [9-15]. Nonetheless, the role of EPS8 in HCC has been never reported, which may partly due to the unobvious difference of mRNA expression between HCC tumor tissues and adjacent non-tumor tissues, and this was further confirmed by our result using the TCGA and GTEx data. Hence, whether other three EPS8Ls would take the place of EPS8 in HCC carcinogenesis was needed to be further investigated. According to the TCGA and GTEx databases, only the mRNA expression of EPS8L3, not EPS8L1 and EPS8L2, showed significant difference between two groups, and the difference was also verified in other five kinds of cancer. Therefore, we chose EPS8L3 for further investigation and to verify whether it had a similar role in carcinogenesis with EPS8. In spite of the unobvious correlation between the mRNA expression of EPS8L3 and other family members, the relationship among the EPS8Ls was still needed to be further explored both in expression and function.

In our present study, we revealed that both the EPS8L3 mRNA expression and protein expression were commonly upregulated in tumor tissues compared with adjacent normal tissues. Furthermore, the overexpression of EPS8L3 was confirmed by the TMAs containing paired tissues of 114 HCC patients. The IHC results also demonstrated that the high EPS8L3 expression was statistically associated with pathological differentiation, and patients with low EPS8L3 expression showed better survival. Only a few of EPS8L3 related studies could be found, and the majority was referred to Marie Unna hereditary hypotrichosis. Hence, our results may provide a novel evidence of aberrant upregulation of EPS8L3 in some kinds of tumor tissues, especially in the HCC tissues.

In term of the functional exploration, we showed that the cell growth was obviously inhibited in HCC cells with EPS8L3 knockdown, and significantly promoted with EPS8L3 overexpression. As unrestricted cell proliferation is considered

to be a major hallmark of cancer [24], EPS8L3 may play an important role in HCC carcinogenesis. In the western blot analysis, we found that the expression of p21 and p27, which were regarded as two major cell cycle regulators, were decreased with EPS8L3 overexpression and increased with EPS8L3 knockdown. In conclusion, these data indicated that EPS8L3 may affect the cell cycle process by modulating the expression of p21 and p27, leading to the promotion of cell proliferation. The finding was consistent with another EPS8L3 related study, which revealed that EPS8L3 could promote cell proliferation by inhibiting the transitivity of FOXO1 [25].

Similarly, the enhanced abilities of migration and invasion were also considered to be major characteristics of cancer. Our study demonstrated that the overexpression of EPS8L3 enhanced both abilities while both were weakened by the knockdown of EPS8L3. As the EPS8 family shared major structure and functional regions, they were believed to have some similarities in regulating cell function. EPS8 was a relatively well-study molecules in the family, and was reported to play an important role in capping the barbed ends of actin filament, leading to the control of actin-based motility in many studies [10, 26-28]. According to our study, the ability of regulating dynamic actin-based cell protrusions and intercellular cytoskeletal organization was appeared to have some difference between EPS8 knockdown groups and control group, but the difference seem to be not obvious enough in the EPS8L3 knockdown groups and control group. These results revealed that the effect of EPS8L3 in regulating cytoskeletal organization was not as efficient as EPS8, and EPS8L3 may promote cell migration and invasion through other ways.

As EPS8L3 has shown an important effect on cell proliferation, migration and invasion, we investigated the underlying molecular mechanisms. EPS8Ls, which regarded as substrates for EGFR, shared an EGFR-binding region [16].
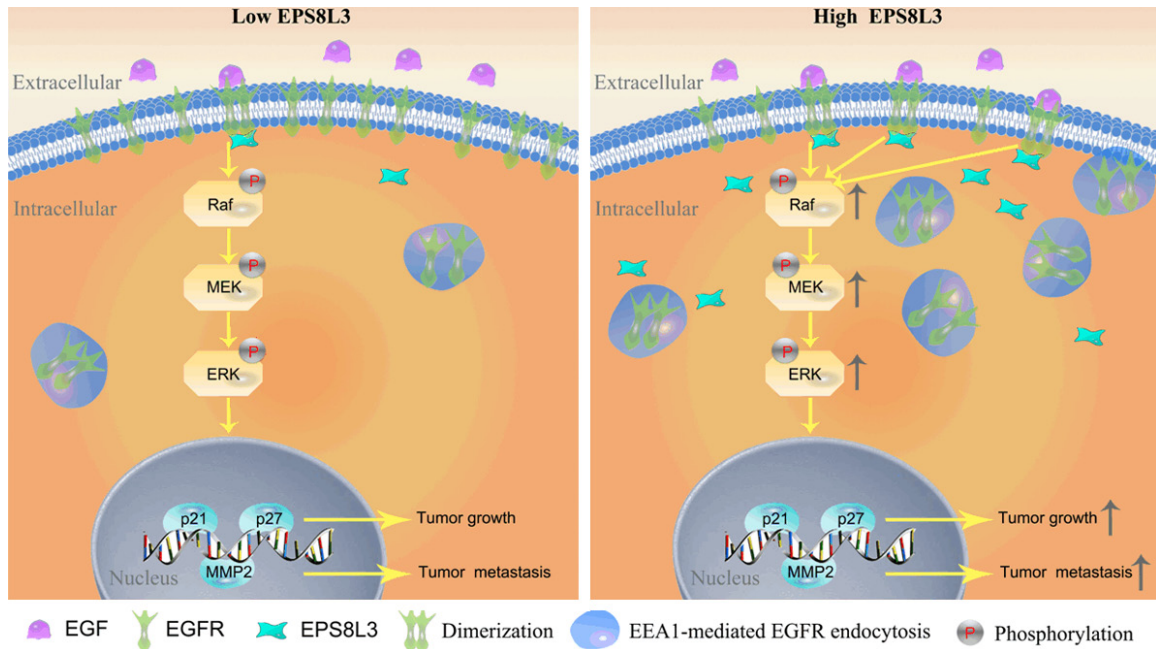
Figure 8. The proposed model for the function and mechanism of EPS8L3 in HCC.

By interacting with EGFR, the EGFR signaling pathways would be modulated, and this was considered to be an important way for various proteins to control the malignant phenotypes of cancer cells [29-32]. As one of the main downstream effectors of EGFR, ERK phosphorylation was significantly inhibited in EPS8L3 knockdown groups comparing with control group, and this process was at least in part through the RAF-MEK-ERK axis. Meanwhile, the protein expression of EPS8 was still unchanged. Consistent with ERK phosphorylation, the protein levels of MMP2, p21 and p27 also changed with the alteration of EPS8L3. Moreover, the change of MMP2 may contribute to the change of the abilities of cell migration and invasion. These results implied that EPS8L3 could affect cell proliferation, migration and invasion presumably by modulating the EGFR-ERK signaling axis.

Dimerization and internalization of EGFR were two key processes following EGFR binding with EGF, as dimerization could initiate the signal transduction [33-35] and EEA1-mediated endocytosis could lead to the EGFR recycling and sustained the signaling [36, 37]. Our recent results demonstrated that EPS8L3 may affect the dimerization and internalization of EGFR, which could subsequently modulate the EGFR signaling cascade.

Results from *in vivo* experiments also revealed that the knockdown of EPS8L3 could reduce the tumor volume and weight, but overexpression of EPS8L3 could increase both. The similar results also appeared in the pulmonary colonization assay, and these results were consistent with the results of *in vitro* experiments. Moreover, IHC analysis indicated that the expression of Ki-67 and MMP2 were decreased with EPS8L3 knockdown, and increased with EPS8L3 overexpression. Hence, our findings suggested that EPS8L3 could affect the tumor growth and pulmonary colonization, and the change of the ability of pulmonary colonization is likely mediated by the alteration of MMP2.

In conclusion, we demonstrated that EPS8L3 could affect the dimerization and internalization of EGFR, and regulate cell proliferation and metastasis probably through the modulation of EGFR-ERK pathway (**Figure 8**). Furthermore, we revealed that EPS8L3 could share some similar functions, but the efficacy was weakened to some extent when compared with EPS8. Hence, our study suggested that overexpressed EPS8L3 not only correlated with HCC prognosis but also led to the promotion of HCC cell proliferation and metastasis, and this may imply that EPS8L3 could become a potential target for the novel and effective treatment of HCC.

Disclosure of conflict of interest

None.

Address correspondence to: Penghong Song and Shusen Zheng, Division of Hepatobiliary and Pancreatic Surgery, Department of Surgery, First Affiliated Hospital, School of Medicine, Zhejiang University, Hangzhou 310003, China. Tel: +86-0571-87236466; Fax: +86-0571-87236466; E-mail: songpenghong@zju.edu.cn (PHS); Tel: +86-0571-87236601; Fax: +86-0571-87236601; E-mail: shusenzheng@zju.edu.cn (SSZ)

References

[1] Bray F, Ferlay J, Soerjomataram I, Siegel RL, Torre LA and Jemal A. Global cancer statistics 2018: GLOBOCAN estimates of incidence and mortality worldwide for 36 cancers in 185 countries. CA Cancer J Clin 2018; 68: 394-424.

[2] Llovet JM, Zucman-Rossi J, Pikarsky E, Sangro B, Schwartz M, Sherman M and Gores G. Hepatocellular carcinoma. Nat Rev Dis Primers 2016; 2: 16018.

[3] Henriksen L, Grandal MV, Knudsen SL, van Deurs B and Grovdal LM. Internalization mechanisms of the epidermal growth factor receptor after activation with different ligands. PLoS One 2013; 8: e58148.

[4] Kan Z, Jaiswal BS, Stinson J, Janakiraman V, Bhatt D, Stern HM, Yue P, Haverty PM, Bourgon R, Zheng J, Moorhead M, Chaudhuri S, Tomsho LP, Peters BA, Pujara K, Cordes S, Davis DP, Carlton VE, Yuan W, Li L, Wang W, Eigenbrot C, Kaminker JS, Eberhard DA, Waring P, Schuster SC, Modrusan Z, Zhang Z, Stokoe D, de Sauvage FJ, Faham M and Seshagiri S. Diverse somatic mutation patterns and pathway alterations in human cancers. Nature 2010; 466: 869-873.

[5] Sorkin A and Goh LK. Endocytosis and intracellular trafficking of ErbBs. Exp Cell Res 2008; 314: 3093-3106.

[6] Rosell R, Carcereny E, Gervais R, Vergnenegre A, Massuti B, Felip E, Palmero R, Garcia-Gomez R, Pallares C, Sanchez JM, Porta R, Cobo M, Garrido P, Longo F, Moran T, Insa A, De Marinis F, Corre R, Bover I, Illiano A, Dansin E, de Castro J, Milella M, Reguart N, Altavilla G, Jimenez U, Provencio M, Moreno MA, Terrasa J, Muñoz-Langa J, Valdivia J, Isla D, Domine M, Molinier O, Mazieres J, Baize N, Garcia-Campelo R, Robinet G, Rodriguez-Abreu D, Lopez-Vivanco G, Gebbia V, Ferrera-Delgado L, Bombaron P, Bernabe R, Bearz A, Artal A, Cortesi E, Rolfo C, Sanchez-Ronco M, Drozdowskyj A, Queralt C, de Aguirre I, Ramirez JL, Sanchez JJ, Molina MA, Taron M and Paz-Ares L; Spanish Lung Cancer Group in collaboration with Groupe Français de Pneumo-Cancérologie and Associazione Italiana Oncologia Toracica. Erlotinib versus standard chemotherapy as first-line treatment for European patients with advanced EGFR mutation-positive non-small-cell lung cancer (EURTAC): a multicentre, open-label, randomised phase 3 trial. Lancet Oncol 2012; 13: 239-246.

[7] Sequist LV, Waltman BA, Dias-Santagata D, Digumarthy S, Turke AB, Fidias P, Bergethon K, Shaw AT, Gettinger S, Cosper AK, Akhavanfard S, Heist RS, Temel J, Christensen JG, Wain JC, Lynch TJ, Vernovsky K, Mark EJ, Lanuti M, Iafrate AJ, Mino-Kenudson M and Engelman JA. Genotypic and histological evolution of lung cancers acquiring resistance to EGFR inhibitors. Sci Transl Med 2011; 3: 75ra26.

[8] Tocchetti A, Confalonieri S, Scita G, Di Fiore PP and Betsholtz C. In silico analysis of the EPS8 gene family: genomic organization, expression profile, and protein structure. Genomics 2003; 81: 234-244.

[9] Maa MC, Lee JC, Chen YJ, Chen YJ, Lee YC, Wang ST, Huang CC, Chow NH and Leu TH. Eps8 facilitates cellular growth and motility of colon cancer cells by increasing the expression and activity of focal adhesion kinase. J Biol Chem 2007; 282: 19399-19409.

[10] Welsch T, Endlich K, Giese T, Buchler MW and Schmidt J. Eps8 is increased in pancreatic cancer and required for dynamic actin-based cell protrusions and intercellular cytoskeletal organization. Cancer Lett 2007; 255: 205-218.

[11] Yap LF, Jenei V, Robinson CM, Moutasim K, Benn TM, Threadgold SP, Lopes V, Wei W, Thomas GJ and Paterson IC. Upregulation of Eps8 in oral squamous cell carcinoma promotes cell migration and invasion through integrin-dependent Rac1 activation. Oncogene 2009; 28: 2524-2534.

[12] Xu M, Shorts-Cary L, Knox AJ, Kleinsmidt-DeMasters B, Lillehei K and Wierman ME. Epidermal growth factor receptor pathway substrate 8 is overexpressed in human pituitary tumors: role in proliferation and survival. Endocrinology 2009; 150: 2064-2071.

[13] Chen H, Wu X, Pan ZK and Huang S. Integrity of SOS1/EPS8/ABI1 tri-complex determines ovarian cancer metastasis. Cancer Res 2010; 70: 9979-9990.

[14] Schoenherr C, Serrels B, Proby C, Cunningham DL, Findlay JE, Baillie GS, Heath JK and Frame MC. Eps8 controls Src- and FAK-dependent phenotypes in squamous carcinoma cells. J Cell Sci 2014; 127: 5303-5316.

[15] Chen C, Liang Z, Huang W, Li X, Zhou F, Hu X, Han M, Ding X and Xiang S. Eps8 regulates cellular proliferation and migration of breast cancer. Int J Oncol 2015; 46: 205-214.

[16] Offenhauser N, Borgonovo A, Disanza A, Romano P, Ponzanelli I, Iannolo G, Di Fiore PP and Scita G. The eps8 family of proteins links growth factor stimulation to actin reorganization generating functional redundancy in the Ras/Rac pathway. Mol Biol Cell 2004; 15: 91-98.

[17] Zhang X, Guo BR, Cai LQ, Jiang T, Sun LD, Cui Y, Hu JC, Zhu J, Chen G, Tang XF, Sun GQ, Tang HY, Liu Y, Li M, Li QB, Cheng H, Gao M, Li P, Yang X, Zuo XB, Zheng XD, Wang PG, Wang J, Wang J, Liu JJ, Yang S, Li YR and Zhang XJ. Exome sequencing identified a missense mutation of EPS8L3 in Marie Unna hereditary hypotrichosis. J Med Genet 2012; 49: 727-730.

[18] Li Q, Liu LH, Chang RX, Pan GB, Chen G, Gao M, Cai LQ, Wang PG, Pimentel JD, Pittelkow MR, Yang S and Zhang XJ. Two cases of Marie Unna hereditary hypotrichosis: clinical features and mutation analysis of the U2HR and EPS8L3 genes. Clin Exp Dermatol 2014; 39: 225-227.

[19] Du Y, Song W, Chen J, Chen H, Xuan Z, Zhao L, Chen J, Jin C, Zhou M, Tuo B, Zhao Y, Zheng S and Song P. The potassium channel KCa3.1 promotes cell proliferation by activating SKP2 and metastasis through the EMT pathway in hepatocellular carcinoma. Int J Cancer 2019; 145: 503-516.

[20] Zhou C, Wu YL, Chen G, Feng J, Liu XQ, Wang C, Zhang S, Wang J, Zhou S, Ren S, Lu S, Zhang L, Hu C, Hu C, Luo Y, Chen L, Ye M, Huang J, Zhi X, Zhang Y, Xiu Q, Ma J, Zhang L and You C. Erlotinib versus chemotherapy as first-line treatment for patients with advanced EGFR mutation-positive non-small-cell lung cancer (OPTIMAL, CTONG-0802): a multicentre, open-label, randomised, phase 3 study. Lancet Oncol 2011; 12: 735-742.

[21] Geyer CE, Forster J, Lindquist D, Chan S, Romieu CG, Pienkowski T, Jagiello-Gruszfeld A, Crown J, Chan A, Kaufman B, Skarlos D, Campone M, Davidson N, Berger M, Oliva C, Rubin SD, Stein S and Cameron D. Lapatinib plus capecitabine for HER2-positive advanced breast cancer. N Engl J Med 2006; 355: 2733-2743.

[22] Ravaud A, Hawkins R, Gardner JP, von der Maase H, Zantl N, Harper P, Rolland F, Audhuy B, Machiels JP, Petavy F, Gore M, Schoffski P and El-Hariry I. Lapatinib versus hormone therapy in patients with advanced renal cell carcinoma: a randomized phase III clinical trial. J Clin Oncol 2008; 26: 2285-2291.

[23] Villanueva A, Hernandez-Gea V and Llovet JM. Medical therapies for hepatocellular carcinoma: a critical view of the evidence. Nat Rev Gastroenterol Hepatol 2013; 10: 34-42.

[24] Hanahan D and Weinberg RA. Hallmarks of cancer: the next generation. Cell 2011; 144: 646-674.

[25] Zeng CX, Tang LY, Xie CY, Li FX, Zhao JY, Jiang N, Tong Z, Fu SB, Wen FJ and Feng WS. Overexpression of EPS8L3 promotes cell proliferation by inhibiting the transactivity of FOXO1 in HCC. Neoplasma 2018; 65: 701-707.

[26] Provenzano C, Gallo R, Carbone R, Di Fiore PP, Falcone G, Castellani L and Alema S. Eps8, a tyrosine kinase substrate, is recruited to the cell cortex and dynamic F-actin upon cytoskeleton remodeling. Exp Cell Res 1998; 242: 186-200.

[27] Disanza A, Carlier MF, Stradal TE, Didry D, Frittoli E, Confalonieri S, Croce A, Wehland J, Di Fiore PP and Scita G. Eps8 controls actin-based motility by capping the barbed ends of actin filaments. Nat Cell Biol 2004; 6: 1180-1188.

[28] Logue JS, Cartagena-Rivera AX, Baird MA, Davidson MW, Chadwick RS and Waterman CM. Erk regulation of actin capping and bundling by Eps8 promotes cortex tension and leader bleb-based migration. Elife 2015; 4: e08314.

[29] Wang RY, Chen L, Chen HY, Hu L, Li L, Sun HY, Jiang F, Zhao J, Liu GM, Tang J, Chen CY, Yang YC, Chang YX, Liu H, Zhang J, Yang Y, Huang G, Shen F, Wu MC, Zhou WP and Wang HY. MUC15 inhibits dimerization of EGFR and PI3K-AKT signaling and is associated with aggressive hepatocellular carcinomas in patients. Gastroenterology 2013; 145: 1436-1448, e1-12.

[30] Chettouh H, Fartoux L, Aoudjehane L, Wendum D, Clapéron A, Chrétien Y, Rey C, Scatton O, Soubrane O, Conti F, Praz F, Housset C, Rosmorduc O and Desbois-Mouthon C. Mitogenic insulin receptor-A is overexpressed in human hepatocellular carcinoma due to EGFR-mediated dysregulation of RNA splicing factors. Cancer Res 2013; 73: 3974-3986.

[31] Ye QH, Zhu WW, Zhang JB, Qin Y, Lu M, Lin GL, Guo L, Zhang B, Lin ZH, Roessler S, Forgues M, Jia HL, Lu L, Zhang XF, Lian BF, Xie L, Dong QZ, Tang ZY, Wang XW and Qin LX. GOLM1 modulates EGFR/RTK cell-surface recycling to drive hepatocellular carcinoma metastasis. Cancer Cell 2016; 30: 444-458.

[32] Zhong L, Liao D, Zhang M, Zeng C, Li X, Zhang R, Ma H and Kang T. YTHDF2 suppresses cell proliferation and growth via destabilizing the EGFR mRNA in hepatocellular carcinoma. Cancer Lett 2019; 442: 252-261.

[33] Lemmon MA and Schlessinger J. Cell signaling by receptor tyrosine kinases. Cell 2010; 141: 1117-1134.

[34] Schmiedel J, Blaukat A, Li S, Knochel T and Ferguson KM. Matuzumab binding to EGFR prevents the conformational rearrangement required for dimerization. Cancer Cell 2008; 13: 365-373.

[35] Piyush T, Chacko AR, Sindrewicz P, Hilkens J, Rhodes JM and Yu LG. Interaction of galectin-3 with MUC1 on cell surface promotes EGFR dimerization and activation in human epithelial cancer cells. Cell Death Differ 2017; 24: 1937-1947.

[36] Avraham R and Yarden Y. Feedback regulation of EGFR signalling: decision making by early and delayed loops. Nat Rev Mol Cell Biol 2011; 12: 104-117.

[37] Dutta S, Roy S, Polavaram NS, Stanton MJ, Zhang H, Bhola T, Hönscheid P, Donohue TM Jr, Band H, Batra SK, Muders MH and Datta K. Neuropilin-2 regulates endosome maturation and EGFR trafficking to support cancer cell pathobiology. Cancer Res 2016; 76: 418-428.

Table S1. Sequences of siRNAs

Name	Sequence
Negative control-sense	5'-UUCUCCGAACGUGUCACGUTT-3'
Negative control-antisense	5'-ACGUGACACGUUCGGAGAATT-3'
siEPS8-1-sense	5'-GCUUGAUGCCAAGGGCAAATT-3'
siEPS8-1-antisense	5'-UUUGCCCUUGGCAUCAAGCTT-3'
siEPS8-2-sense	5'-GCGAGAGUCUAUAGCCAAATT-3'
siEPS8-2-antisense	5'-UUUGGCUAUAGACUCUCGCTT-3'
siEPS8L3-1-sense	5'-GCUGGACUCUUACCGCCUATT-3'
siEPS8L3-1-antisense	5'-UAGGCGGUAAGAGUCCAGCTT-3'
siEPS8L3-2-sense	5'-CCACCUGAGAGUAACCUUUTT-3'
siEPS8L3-2-antisense	5'-AAAGGUUACUCUCAGGUGGTT-3'

Table S2. The shRNA target sequences for EPS8L3-knockdown

Name	Target Sequences
shRNA1	5'-GGTTCCAATGCTTCGACTTAG-3'
shRNA2	5'-GGAGCCAGCTACTTCGCATAA-3'

Table S3. Primers in realtime-PCR

Name	Primer sequence
EPS8-F	5'-AGTATCGTGCGAGACAGCCAGA-3'
EPS8-R	5'-CTCCGACCAATGGTCAGTCTGT-3'
EPS8L1-F	5'-CTCCACGTGAAAACGAGCTCTG-3'
EPS8L1-R	5'-CGCTGAAGAACTCGGGTCTGTA-3'
EPS8L2-F	5'-CAAGGACCTGTTTGAGCAGAGG-3'
EPS8L2-R	5'-GTGATGGCTTCGCTCTTGTCCA-3'
EPS8L3-F	5'-CTGCTACAGTCCTGTCTAAGCC-3'
EPS8L3-R	5'-GAGAATGTGGGTTGGTAGGGCA-3'
GAPDH-F	5'-GAGCCAAAAGGGTCATCATCT-3'
GAPDH-R	5'-TTCCACGATACCAAAGTTGTCA-3'
ALB-F	5'-GATGAGATGCCTGCTGACTTGC-3'
ALB-R	5'-CACGACAGAGTAATCAGGATGCC-3'
CK18-F	5'-GCTGGAAGATGGCGAGGACTTT-3'
CK18-R	5'-TGGTCTCAGACACCACTTTGCC-3'
C/EBPα-F	5'-AGGAGGATGAAGCCAAGCAGCT-3'
C/EBPα-R	5'-AGTGCGCGATCTGGAACTGCAG-3'
HNF1α-F	5'-AGACGCTAGTGGAGGAGTGCAA-3'
HNF1α-R	5'-GGCAAACCAGTTGTAGACACGC-3'
SOX-F	5'-GCTACAGCATGATGCAGGACCA-3'
SOX-R	5'-TCTGCGAGCTGGTCATGGAGTT-3'
BMI1-F	5'-GGTACTTCATTGATGCCACAACC-3'
BMI1-R	5'-CTGGTCTTGTGAACTTGGACATC-3'
OCT4-F	5'-CCTGAAGCAGAAGAGGATCACC-3'
OCT4-R	5'-AAAGCGGCAGATGGTCGTTTGG-3'
NANOG-F	5'-CTCCAACATCCTGAACCTCAGC-3'
NANOG-R	5'-CGTCACACCATTGCTATTCTTCG-3'
ZO1-F	5'-GTCCAGAATCTCGGAAAAGTGCC-3'

ZO1-R	5'-CTTTCAGCGCACCATACCAACC-3'
CDH1-F	5'-CTCACATTTCCCAACTCCTCTC-3'
CDH1-R	5'-ACCTTGCCTTCTTTGTCTTTGT-3'
CDH2-F	5'-CCTCCAGAGTTTACTGCCATGAC-3'
CDH2-R	5'-GTAGGATCTCCGCCACTGATTC-3'
VIMENTIN-F	5'-ATCCAAGTTTGCTGACCTCTCT-3'
VIMENTIN-R	5'-GTTCTCTTCCATTTCACGCATC-3'
SNAIL-F	5'-CAATCGGAAGCCTAACTACAGC-3'
SNAIL-R	5'-ACAGAGTCCCAGATGAGCATT-3'
SLUG-F	5'-ATCTGCGGCAAGGCGTTTTCCA-3'
SLUG-R	5'-GAGCCCTCAGATTTGACCTGTC-3'
TWIST-F	5'-GCCAGGTACATCGACTTCCTCT-3'
TWIST-R	5'-TCCATCCTCCAGACCGAGAAGG-3'
ZEB1-F	5'-CAGTGAAAGAGAAGGGAATGCT-3'
ZEB1-R	5'-TACATCCTGCTTCATCTGCCT-3'

Table S4. Antibodies for immunohistochemistry, immunofluo-
rescence and western blot analysis

| Antibody	Catalog Number	Manufacturer
EPS8L3	ab196678	Abcam
EEA1	ab196186	Abcam
EGFR	ab30	Abcam
ERK1/2	ab54230	Abcam
pERK1/2	ab76299	Abcam
Raf-1	ab137435	Abcam
pRaf-1	ab173539	Abcam
MEK1	ab32091	Abcam
pMEK1	ab96379	Abcam
Ki-67	ab15580	Abcam
SOS1	ab140621	Abcam
ABI1	ab233412	Abcam
EPS8	ab124882	Abcam
EPS8	#43114	Cell Signaling Technology
EGFR	#4267	Cell Signaling Technology
pEGFR	#3777	Cell Signaling Technology
E-Cadherin	#3195	Cell Signaling Technology
N-Cadherin	#13116	Cell Signaling Technology
Vimentin	#5741	Cell Signaling Technology
MMP9	#13667	Cell Signaling Technology
MMP2	#40994	Cell Signaling Technology
p27	#3686	Cell Signaling Technology
p21	#2947	Cell Signaling Technology
p27	25614-1-AP	Proteintech
GAPDH	10494-1-AP	Proteintech
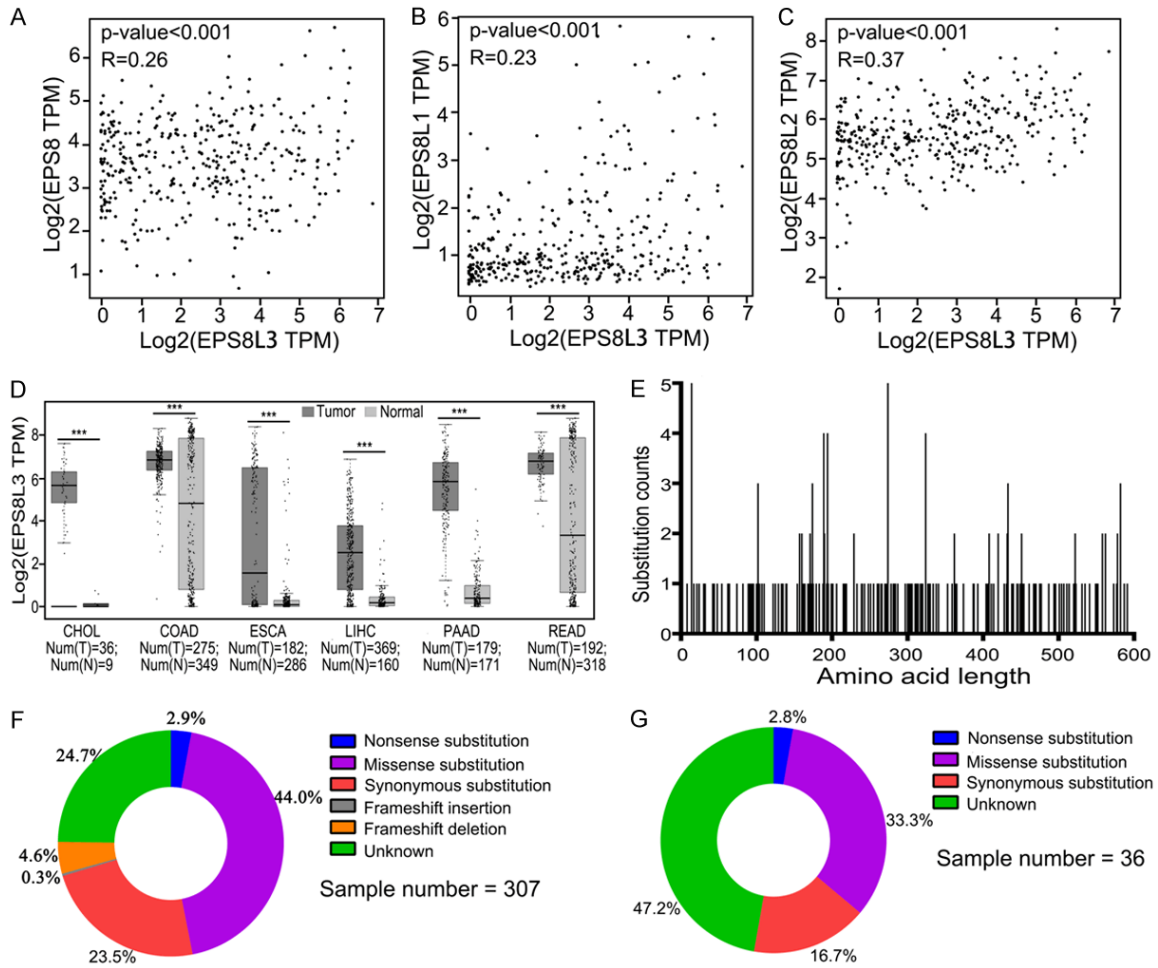
Figure S1. The mRNA expression of EPS8Ls family and the mutations of EPS8L3. A-C. The correlation between the mRNA expression of EPS8L3 and other three family members of human HCC tissues in TCGA database (N = 369). D. The mRNA expressions of EPS8L3 were evaluated in five kinds of tumor tissues apart from HCC comparing with respective normal tissues in TCGA and GTEx databases. CHOL: Cholangiocarcinoma; COAD: Colon adenocarcinoma; ESCA: Esophageal carcinoma; LIHC: Liver hepatocellular carcinoma; PAAD: Pancreatic adenocarcinoma; READ: Rectum adenocarcinoma. E. Graphical view of mutations across EPS8L3 in pan-cancer samples. Mutations are displayed at the amino acid level across the full length of the gene. F, G. The composition of point mutations in pan-cancer samples and liver cancer samples. *: P<0.05, **: P<0.01, ***: P<0.001.
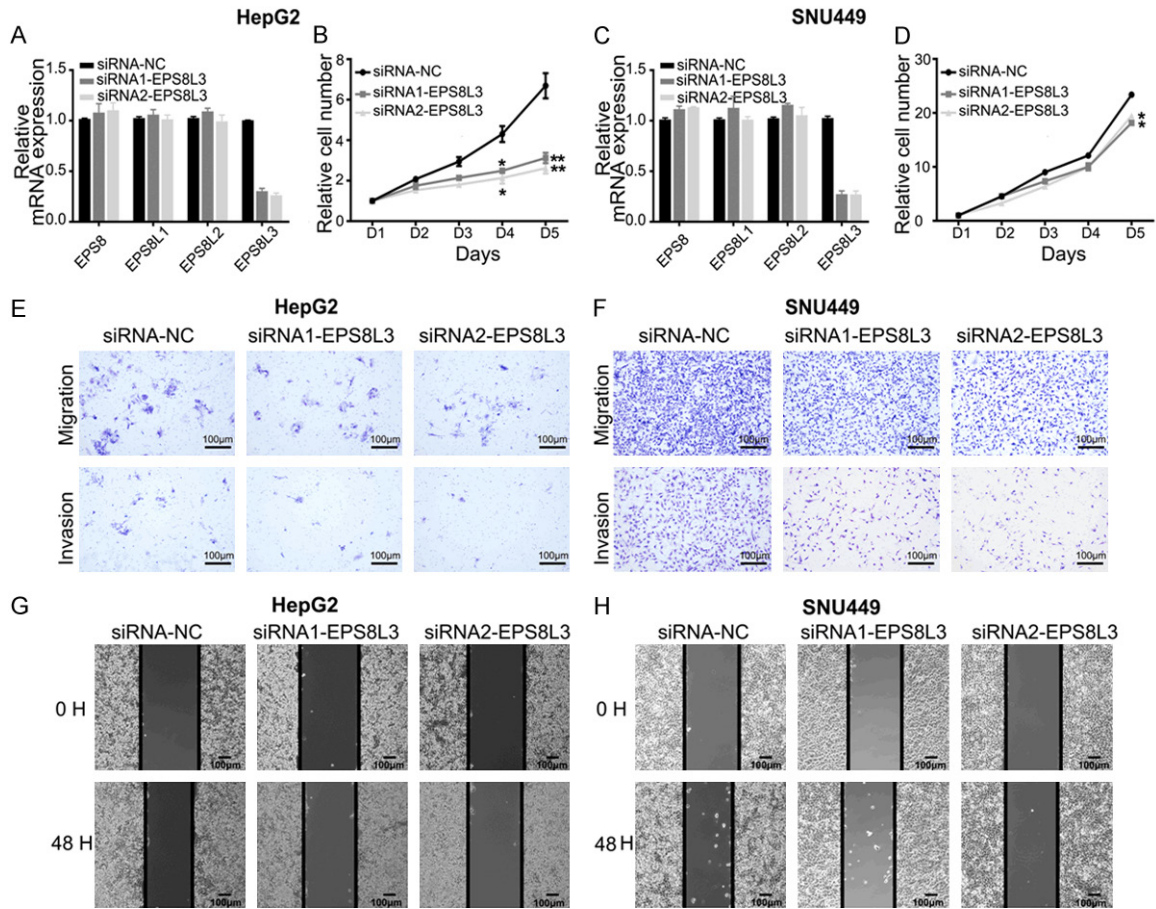
Figure S2. EPS8L3 affects cell proliferation, migration and invasion in HCC cells. A, B. The relative mRNA expression of EPS8Ls family and cell growth after EPS8L3 knockdown in HepG2 cells. C, D. The relative mRNA expression of EPS8Ls family and cell growth after EPS8L3 knockdown in SNU449 cells. E, F. The migratory and invasive abilities of HepG2 and SNU449 cells were evaluated by transwell assays. Representative images were shown. G, H. Representative images of wound healing assay using HepG2 and SNU449 cells. Results of three independent experiments were shown as mean ± s.d. *: P<0.05, **: P<0.01.
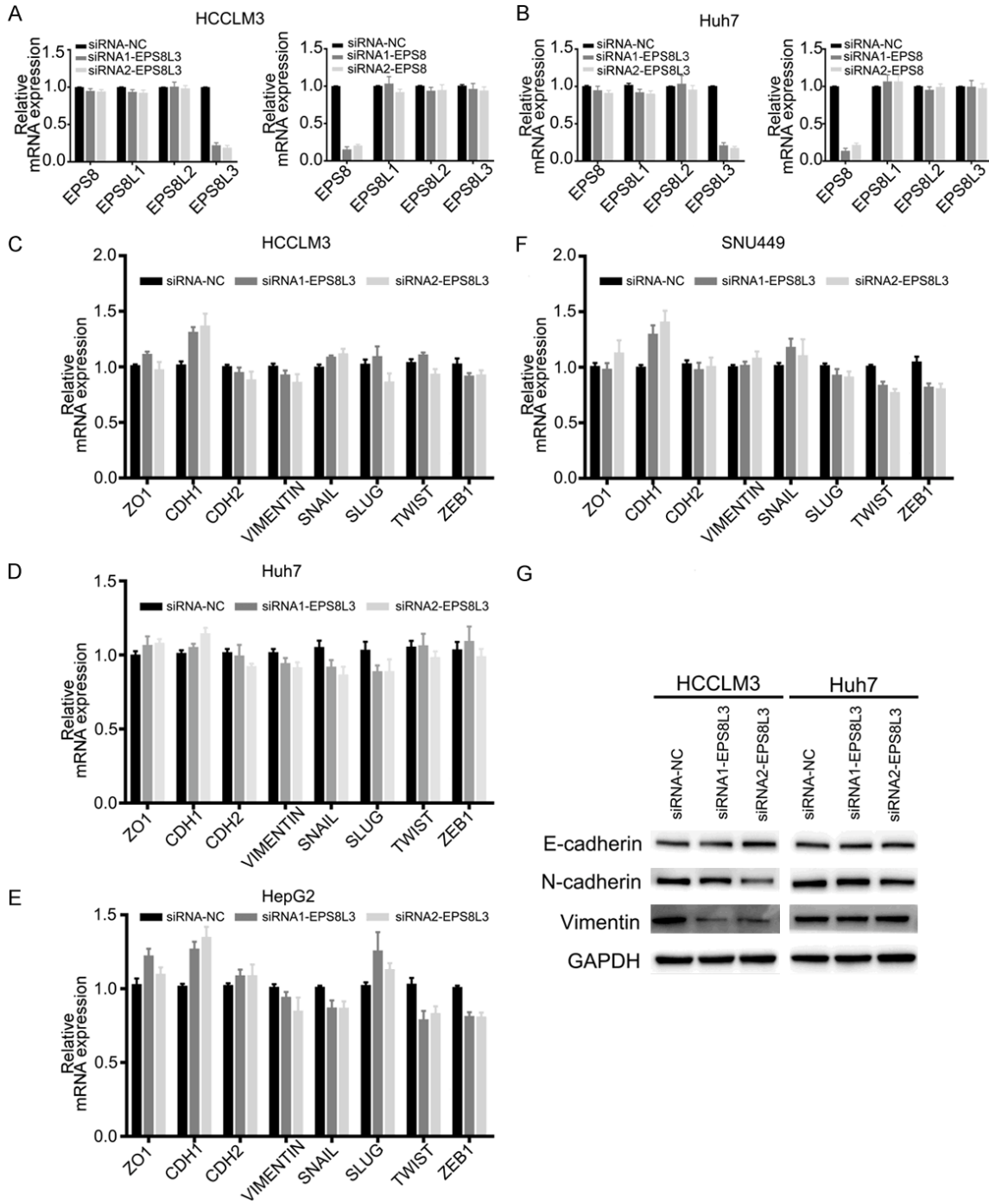
Figure S3. The expression changes of EPS8Ls and EMT related genes after EPS8L3 knockdown. (A, B) The relative mRNA expression of EPS8Ls family after EPS8L3 or EPS8 knockdown in HCCLM3 (A) and Huh7 (B) cells. (C-F) The relative mRNA expression of EMT related genes after EPS8L3 knockdown in HCCLM3, Huh7, HepG2 and SNU449 cells. (G) The protein expression of E-cadherin, N-cadherin and Vimentin after EPS8L3 knockdown in HCCLM3 and Huh7. Results of three independent experiments were shown as mean ± s.d.
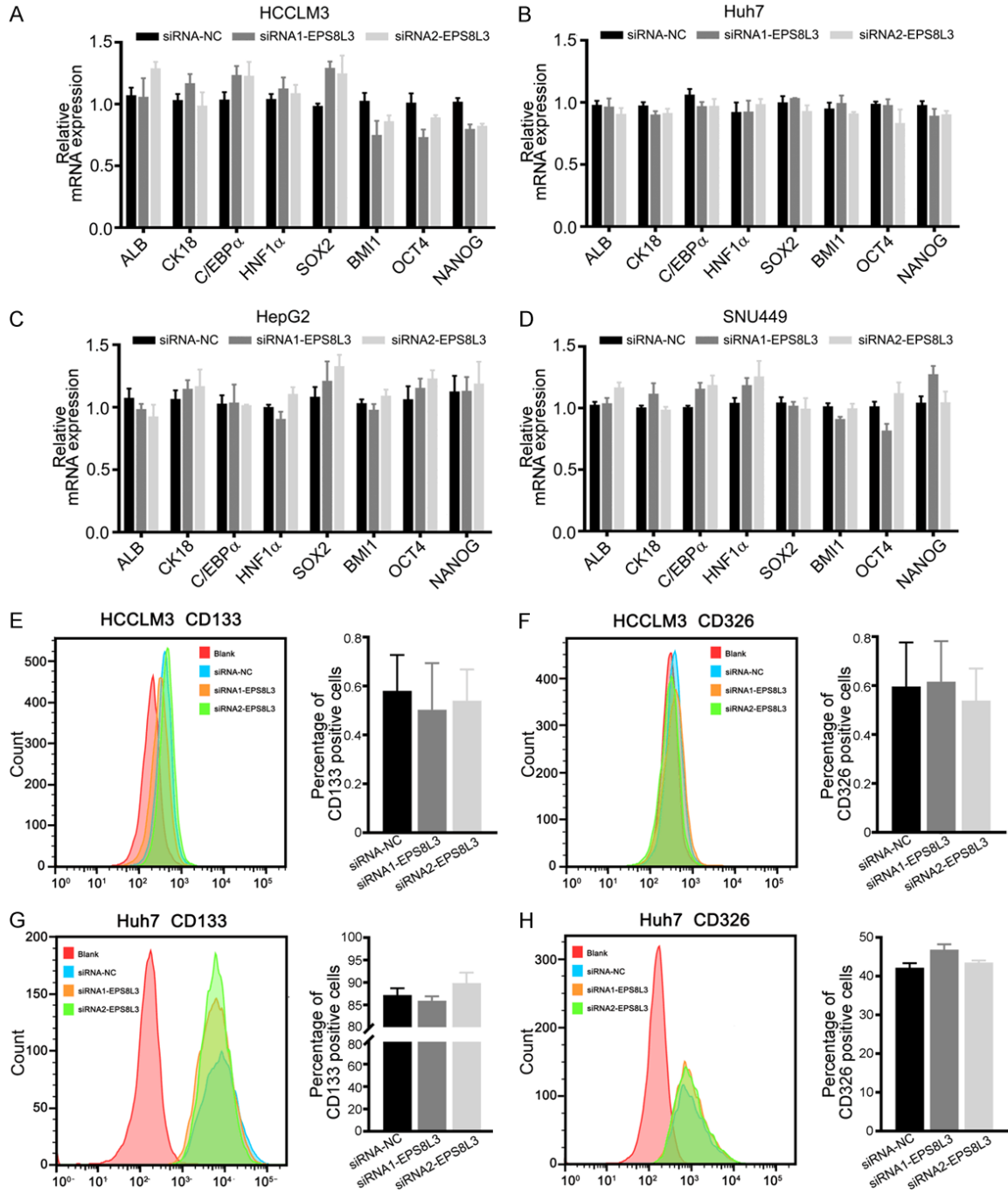
Figure S4. The change of cell stemness and hepatic differentiation related markers after EPS8L3 knockdown. A-D. The relative mRNA expression of cell stemness and hepatic differentiation related markers after EPS8L3 knockdown in HCCLM3, Huh7, HepG2 and SNU449 cells. E, F. The percentages of CD133 and CD326 positive cells were evaluated by flow cytometry in HCCLM3 cells. Representative images were shown. G, H. The percentages of CD133 and CD326 positive cells were evaluated by flow cytometry in Huh7 cells. Representative images were shown. Results of three independent experiments were shown as mean ± s.d.